Self-force scattering in the strong and weak field

arXiv:2406.08363

Chris Whittall
with Oliver Long & Leor Barack

27th Capra Meeting
National University of Singapore
17th June 2024

Scalar-field self-force and scattering: recap

- Scatter orbits parameterised by velocity at infinity v and impact parameter $b > b_c(v)$.

- Using scalar-field toy model in Schwarzschild

$$\nabla\Phi = -4\pi q \int \frac{\delta^4(x^\alpha - x_p^\alpha(\tau))}{\sqrt{-g}} d\tau,$$
$$u^\beta \nabla_\beta u^\alpha = q(g^{\alpha\beta} + u^\alpha u^\beta)\nabla_\beta \Phi^R := \epsilon F^\alpha,$$

where $\epsilon := q^2/\mu M \ll 1$ is the expansion parameter.

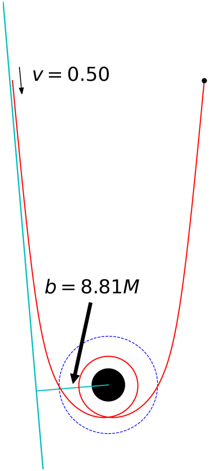

SF scatter angle correction

- Scatter angle expanded

$$\chi(v, b) = \chi^{0\mathrm{SF}}(v, b) + \epsilon\chi^{1\mathrm{SF}}(v, b) + O(\epsilon^2),$$

- Split between geodesic term $\chi^{0\mathrm{SF}}$ and self-force *correction* $\chi^{1\mathrm{SF}}$ defined at fixed (v, b).

- 1SF correction expressed as integral of SF along background geodesic [Barack & Long 22]

$$\chi^{1\mathrm{SF}} = \int_{-\infty}^{+\infty} \left[\mathcal{G}_E(\tau)F_t(\tau) - \mathcal{G}_L(\tau)F_\varphi(\tau)\right] d\tau$$

Numerical platforms

- **Time-domain** code (see previous talk by O. Long):
  - Finite differences, null grid.
  - Performed first calculations of $\chi^{1\mathrm{SF}}$ in [Barack & Long 22].
  - Typically limited to $\ell_{\max} = 15$.

- **Frequency-domain** code:
  - SF reconstructed from frequency modes of an extended homogeneous solution.
  - Highly accurate near periapsis, access to at least $\ell_{\max} = 25$.
  - Loss of precision for large-ℓ modes at larger radii; $\ell_{\max}$ must be reduced rapidly.

FD code more accurate than TD in strong-field, but loses precision at larger radii

PM expansion of χ^{1SF}

Analytical progress using post-Minkowskian expansion,

$$\chi^{\mathrm{1SF}} = \sum_{k=2}^{\infty} \chi_k^{\mathrm{1SF}}(v) \left(\frac{GM}{b}\right)^k .$$

- Coefficients known through 4PM order for scalar-field. [Gralla & Lobo 22, Barack & Long 22, Barack et al 23, Bini et al 24]
- Good agreement found with numerical self-force. [Barack et al 23]
- Since then, χ_4^{cons} determined completely using PM/PN calculation (see talk by D. Usseglio after coffee break).

1SF correction: examples

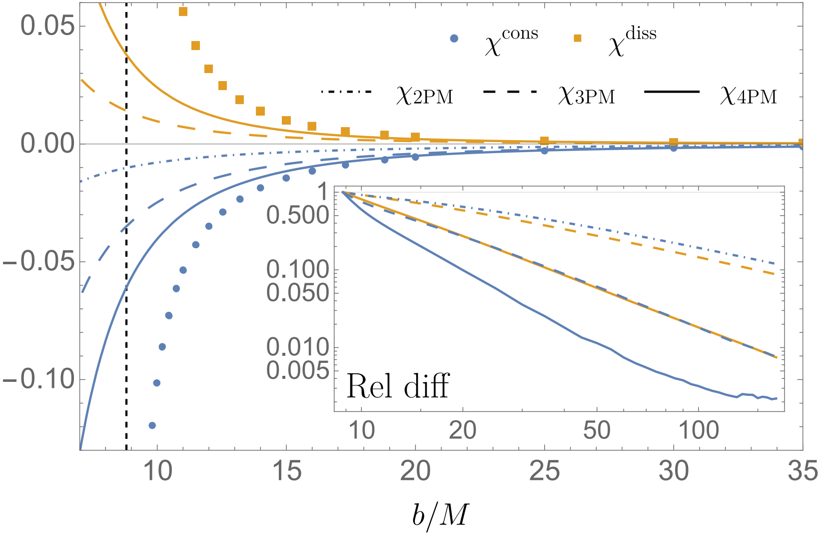

Figure: comparison between numerical SF scatter angles and successive PM approximations ($v = 0.5$)

Transition to plunge

- Separatrix $b = b_c(v)$ divides scatter $(b > b_c(v))$ from plunge $(b < b_c(v))$.
- Each critical "geodesic" $b = b_c(v)$ has two branches:
  - **Inbound:** begins at infinity, is captured into circular orbit.
  - **Outbound:** begins as circular orbit, escapes to infinity.
- Conservative/dissipative forces obtained from combinations of SF along inbound/outbound branches.

$$\delta b := b - b_c(v)$$

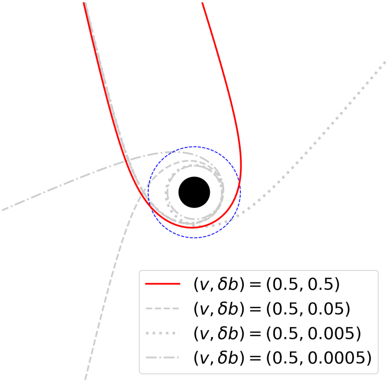

Figure: scatter geodesics in the $b \to b_c(v)$ limit.

Singularity structure of $\chi^{\rm 0SF}$ and $\chi^{\rm 1SF}$

- Log divergence in $\chi^{\rm 0SF}$:

$$\chi^{0SF} \sim A_0(v)\log\left(\frac{\delta b}{b_c(v)}\right) \text{ as } b \to b_c(v),$$

where, recall, $\delta b := b - b_c(v)$, and

$$A_0(v) = -\left(1 - \frac{12M^2(1-v^2)}{v^2 b_c(v)^2}\right)^{1/2}.$$

- Faster divergence at 1SF,

$$\chi^{1SF} \sim A_1(v)\frac{b_c(v)}{\delta b},$$

as $b \to b_c(v)$.

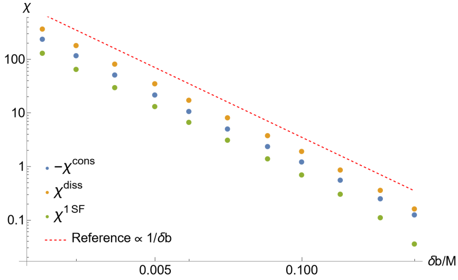

Integral expression for $A_1(v)$ along critical orbit

Divergence parameters $A_1^{\mathrm{cons/diss}}(v)$ can be expressed

$$A_1^{\mathrm{cons}}(v) = -\frac{1}{b_c(v)} \int_{-\infty}^{+\infty} \left(c_E F_t^{\mathrm{cons}} + c_L F_\varphi^{\mathrm{cons}}\right) d\tau,$$

$$A_1^{\mathrm{diss}}(v) = \frac{1}{b_c(v)} \int_{-\infty}^{+\infty} \left(c_E F_t^{\mathrm{diss}} + c_L F_\varphi^{\mathrm{diss}}\right) d\tau,$$

where the integrals and self-forces are evaluated on the *outbound* critical orbit and $c_{E/L}$ are constants.

- Calculation confirms $1/\delta b$ divergence analytically.
- For each v, $A_1^{\mathrm{cons}}(v)$ and $A_1^{\mathrm{diss}}(v)$ obtained by SF calculation along only 2 orbits.
- Current codes unable to calculate SF along critical orbit. Use extrapolation from $b > b_c(v)$ instead.

SF-informed PM resummation

- Introduce

$$\Delta\chi(v,b) := A_0 \left[\log\left(1 - \frac{b_c(v)(1-\epsilon A_1/A_0)}{b}\right) + \sum_{k=1}^{4} \frac{1}{k}\left(\frac{b_c(v)(1-\epsilon A_1/A_0)}{b}\right)^k \right].$$

  - $\Delta\chi = O(b^{-5})$ as $b \to \infty$
  - Matches the $b \to b_c(v)$ divergences of $\chi(v,b)$ at both 0SF and 1SF.

- Resummed scatter angle:

$$\tilde{\chi}(v,b) := \chi_{\mathrm{4PM}}(v,b) + \Delta\chi(v,b).$$

  - Matches $b \to \infty$ behaviour of χ through 4PM order.
  - Matches $b \to b_c(v)$ behaviour at 0SF and 1SF.

- Similar to geodesic order approach introduced in [Damour & Rettegno 2023], but extended to 1SF.

High-velocity limit

- Large-ℓ modes become more important at high velocities.
- Delayed transition to asymptotic behaviour in mode-sum.
    - Possibly associated with relativistic beaming.
- $\ell > 15$ modes can contribute up to a few percent of the total SF.

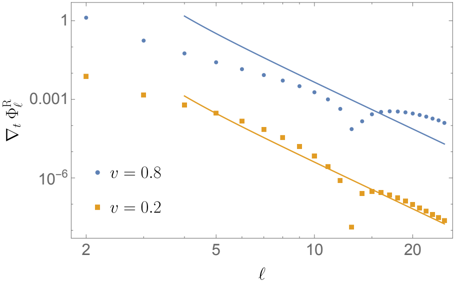

Figure: regularised ℓ-mode contributions to $\nabla_t \Phi^R$ at given points along example low and high velocity orbits.

- Effect largest near periapsis, where FD code can handle $\ell_{\max} > 15$.
- Motivated development of TD/FD hybrid approach.

Hybrid TD-FD model

Hybridisation at the level of the data:

- Run TD and FD codes separately.
- FD code output contains the value of $\ell^{\mathrm{FD}}_{\mathrm{max}}$ at each sample position along the orbit.
- FD self-force data used in region $r_p \leq r_{\mathrm{switch}}$ where $\ell^{\mathrm{FD}}_{\mathrm{max}} \geq 15$.
- TD data used elsewhere.

Figure: F_t along the orbit $(v, b) = (0.7, 6.71307M)$ as calculated using the TD, FD and hybrid methods.

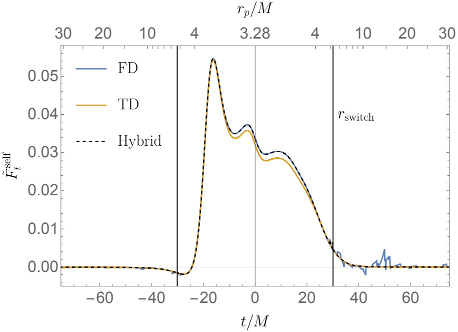

Hybrid approach utilises the most accurate method in each region to construct an optimal SF data set.

Calculating $A_1(v)$ by extrapolation

- Calculate $A_1(v)$ by extrapolating along sequence of ~ 10 orbits with $b \to b_c(v)$ at fixed v.
- More accurate to fit for $A_1^{\mathrm{cons/diss}}(v)$ separately.

Figure: fit models $A_1(v)b_c(v)/\delta b$ for $v = 0.5$.

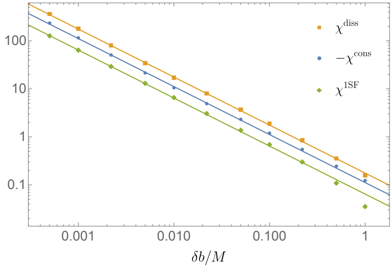

- Fits performed in Mathematica, weighting each scatter angle by $1/\epsilon_{\mathrm{num}}^2$.
- Effect of varying number of points included in fit: investigated and incorporated into error bars on $A_1^{\mathrm{cons/diss}}$.

Results for $A_1(v)$ [OL, CW & LB 2406.08363]

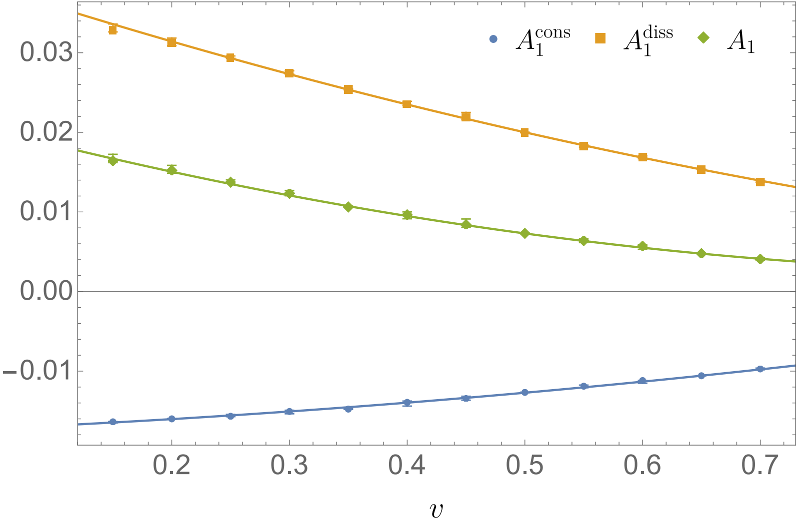

Figure: numerical results for $A_1(v)$ with quadratic best fit functions $A_1(v) \sim a + bv + cv^2$.

Resummation: 1SF scatter angle correction [OL, CW & LB 2406.08363]

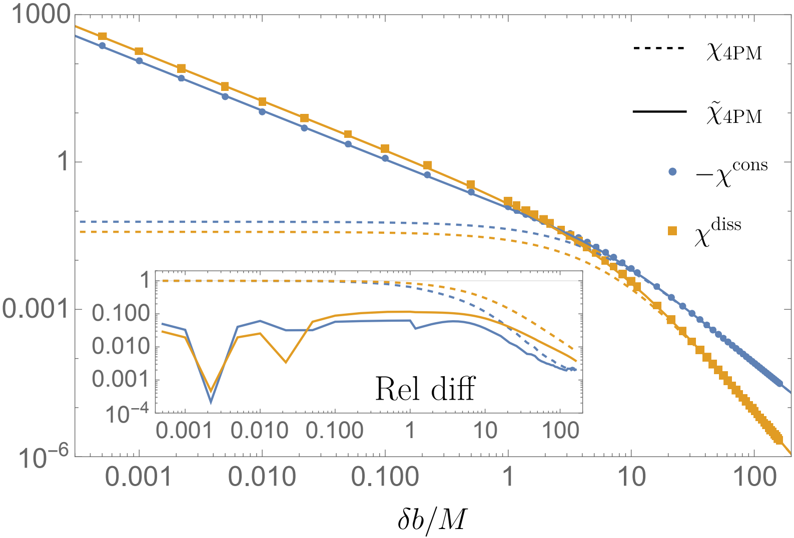

Figure: the resummation procedure significantly improves agreement with the numerical SF data, even in the weak-field. ($v = 0.5$)

Resumation: total scatter angle [OL, CW & LB 2406.08363]

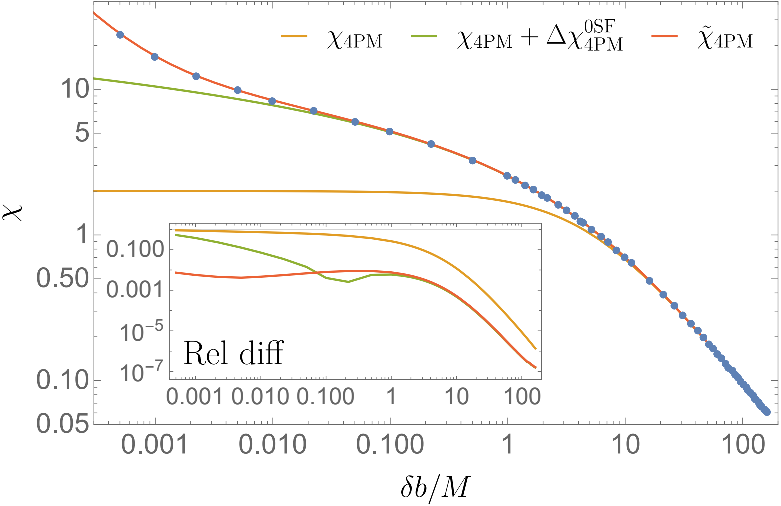

Figure: $\chi^{0\mathrm{SF}} + 0.1\chi^{1\mathrm{SF}}$ for $v = 0.5$. Our 1SF resummation improves upon the geodesic order resummation in the $\delta b \to 0$ limit.

Summary and outlook

Resummed PM provides semi-analytical model which is fast to evaluate and accurate in both strong and weak-field at 1SF.

Next steps:

- Direct calculation of $A_1(v)$ as integral over critical orbit should increase accuracy and decrease computational burden.
- Framework easily extends to gravity once GSF available.
- Ongoing work to obtain analytical results for SF at large radius.